Optical Modeling of the
RIT-Yale Tip-Tilt Speckle Imager Plus

Thesis

Kevin R. Beaulieu

Advisor: Dr. Elliott Horch
Chester F. Carlson Center for Imaging Science
Rochester Institute of Technology
May 2002

Acknowledgements

<u>Elliott Horch</u>   For assisting in all aspects of this senior research and giving me valuable advice as I prepare for a transition from academia to the workplace.

<u>Reed Meyer</u>   For allowing me to utilize his laboratory throughout the year for research needs and answering questions regarding RYTSI.

<u>Robert MacIntyre</u>   For generously providing me an OSLO® Premium license for use throughout the year.

Abstract

Traditionally, speckle imaging has been done with intensified imaging systems such as intensified-CCD (ICCD) and multi-anode microchannel array (MAMA) detectors and has been a popular technique among astronomers for obtaining diffraction-limited images of celestial objects in the presence of atmospheric turbulence. At RIT, the use of large-format CCD detectors for speckle work has been pioneered, but most high-quality CCDs have long read-out times. In CCD-based speckle imaging, astronomers must deal with dead time as a primary consequence of the slow CCD readout speeds. In this project, the optics of a new speckle imaging system, RYTSI-Plus, is modeled in OSLO® and will serve as an upgrade to the original RYTSI for use at the WIYN Observatory for diffraction-limited speckle imaging with little to no observation dead time. The RYTSI-Plus model differs from the original model in that it incorporates two high-efficiency, low-noise CCD detectors, shorter focal length collimating and reimaging lenses, and a "flip" mirror. The "flip" mirror, when active, deflects the light onto one CCD chip as the other "full" CCD reads out. We have determined that although longer focal length lenses would result in more desirable spot diagrams and point spread functions, the optimal collimating and reimaging lens focal lengths for use in RYTSI-Plus, given spatial constraints, are 40mm and 120mm, respectively. The RYTSI-Plus OSLO® optics model will be presented along with analysis of the resulting effects at the image plane.

Introduction

Since the long-term objective of the RYTSI-Plus research is to successfully construct and implement a low noise, high efficiency astronomical data collection system, the optical modeling of the RYTSI-Plus is an extremely important aspect in the development process. By modeling the optics of the new system, Dr. Elliott Horch and Reed Meyer thus have accurate data supporting the selection of specific lenses to be installed in the RYTSI-Plus system.

As a result of this RYTSI-Plus project, the expectation is to be able to decrease astronomical data collection dead time at observatories while obtaining diffraction-limited, low-noise images. After construction, once the system has proved to be accurate and efficient, astronomical research will be conducted using the RYTSI-Plus at the WIYN Observatory at Kitt Peak, Arizona, primarily to study binary stars via speckle imaging methods.

The new RYTSI-Plus system is modeled using the Lambda Research software package, Optics Software for Layout and Optimization of optical systems, OSLO®. The software has been obtained generously through Robert MacIntyre, an adjunct professor at the Chester F. Carlson Center for Imaging Science. "OSLO® is used primarily to determine the optimum sizes and shapes of the elements in optical systems in cameras, consumer products, communications systems, military/space applications, scientific instruments, etc. In addition, it is used to simulate the performance of optical systems, and to develop specialized software tools for optical design, testing, and manufacturing" (http://www.lambdares.com/products/oslo/index.phtml).

In monochromatic optical systems, such as RYTSI-Plus, point spread functions and spot diagrams become extremely important in image quality analysis. First, as with all optical systems, since the distribution of light is spread across the detector, the point spread functions which describe the RYTSI-Plus performance at two different positions on the CCD plane must be acceptable. Next, if the aberrations in the system exceed the Rayleigh limit, diffraction becomes relatively insignificant and geometric raytracing may be used to predict the appearance of a point source with a fair degree of accuracy. To generate a spot diagram, the entrace pupil is divided into an equally spaced grid. Rays are traced through the points on the grid, through the system, and onto the image plane. The image created as a result of all rays which travel through the entrance pupil in this fashion are collectively known as the spot diagram. Each spot on the diagram represents a fraction of the total energy in the image. There is an unavoidable physical limit on the resolution of an image due to the wave nature of light known as the diffraction limit. Thus, spot diagrams are not complete until the diffraction limit is plotted over it, indicating the limit of resolution. In this research, OSLO® has been a useful tool in studying the image quality performance of the new RYTSI-Plus models.

Finally, longer focal length lenses yield higher resolution images because of the decrease in aberrations. Thus, longer focal length lenses yield better point spread functions and spot diagrams. This is realized in this research as the image quality via the use of longer focal length lenses is tested against the image quality via the use of a set of smaller focal length lenses within the RYTSI-Plus models.

Background

Speckle imaging has long been a popular method for obtaining diffraction-limited images affected by atmospheric turbulence. Since 1970, speckle imaging has been used to derive diffraction-limited images of various objects including binary stars, asteroids, planets, young stars, and brown dwarfs. However, speckle imaging places strict requirements on the imaging system; the frame readout time is approximately 30 to 100 frames per second for reasonable observing conditions. CCDs in the late 1970s and early 1980s were not compatible with the speckle imaging method since they had such slow readout rates and high readout noise. Various cameras had been used for speckle imaging at that time. Intensified CCDs, PAPA detectors, resistive anode detectors, and wedge-and-strip detectors have all been useful in imaging bright objects. Although expensive and technologically challenging, adaptive optics allows high-resolution astronomical images to be collected onto the CCDs, which results in higher quantum efficiency.

Since 1997, Rochester Institute of Technology has been using CCDs in speckle imaging as part of a solid-state detector program. The camera that has been used, a Kodak KAF-4200 CCD, is a front-illuminated CCD with a readout rate of 500 kHz and a root-mean-square read noise of approximately 10 electrons. The software package which controls this system, PMIS, allows the astronomer to read out sub-arrays of the chip, execute charge transfer commands, and operate the camera shutter. Since some CCDs do not have these charge transfer capabilities, Zoran Ninkov and William van Altena proposed the creation of a "tip-tilt" speckle imager, which could be used with any CCD camera and would increase efficiency. Using the method, a tip-tilt mirror would deflect the image onto all areas of the CCD, using the CCD as a memory cache of previous speckle images. However, the final product, the RIT-Yale Tip-Tilt Speckle Imager (RYTSI (pronounced- rit Zee))(2001) is still inefficient, because the system uses only one CCD, resulting in a significant amount of dead time during readout. Thus, the *new* system to be modeled, the **RYTSI-Plus**, incorporates *two* high-speed, low-readout noise CCDs and a "flip" mirror for ray deflection, in effect, eradicating this dead observing time.

Methods

The optical modeling process implemented in this project is encapsulated by the following three chronological elements:

I.   *Planning*
        This RYTSI-Plus model will be intended for use at the Kitt Peak WIYN Observatory's Nasmyth port. However, if needed, it will have the capacity to be easily modified for use at the Cassegrain port. A main objective of this research is to model the system such that the spatial dimensions of the housing are ultimately kept to a minimum, yet the optics within yield acceptable image quality at the CCD plane. Thus, the housing dimensions of RYTSI-Plus must obey the strict spatial constraints at the Cassegrain port; the reimaging lens **cannot** be any greater than 120mm. Secondly, due to the bracket which holds it in place, the collimating lens **cannot** be any smaller than 40mm. If the collimating lens focal length were any smaller, the wall on the side of the shutter would have to be extended. Given these constraints, it became evident that the ideal lens combination to utilize in the OSLO® models would be the 40mm collimating, 120mm reimaging lenses. Understanding the above constraints of the system led to the decisions to select lenses in the OSLO® optical models.

II.   *Lens Selections and Modeling*
        While maintaining equal magnification (the ratio of the focal length of the collimating lens to the focal length of the reimaging lens), the next step is to model the RYTSI-Plus system with two collimating and reimaging lens focal length combinations. First, RYTSI-Plus is modeled using the smallest focal length lenses allowed given the spatial constraints (40mm, 120mm) as stated in I. Second, RYTSI-Plus is then modeled using larger focal length lenses (60mm, 180mm) to compare the possible achievable image plane results, ignoring such spatial constraints. Even though the larger focal length lenses would not be used in the final design, it would be useful to study how point spread functions and spot diagrams are affected via the use of larger focal length lenses. In theory, aberrations should decrease as the focal lengths increase; thus, modeling RYTSI-Plus using the two lens focal length combinations is appropriate in analyzing how image quality is affected by the optical modeling within the system.

III.   *Image Plane Analysis / Comparison*
        Using the two lens focal length combinations (40mm collimating, 120mm reimaging; 60mm collimating, 180mm reimaging), the point spread functions and spot diagrams that result at the image plane are analyzed. The following questions are then asked as OSLO® modeling proceeds: Can *acceptable* point spread functions and spot diagrams be obtained using the 40mm, 120mm lens combination for on-axis, raster-mimicking, and "flip" mirror active models? How does an increase in the focal lengths of the two lenses affect image quality?

Results

FINAL MODELS: *40mm collimating /120mm reimaging lens combination*

The following final four optical models for RYTSI-Plus incorporate both on-axis and raster-mimicking scenarios. Melles Griot® doublets were selected from the lens catalogue within OSLO®. It is important to note that the "tip-tilt" mirror is being described as a single reflective surface in the OSLO® models shown below. However, the reflective surface, in actuality, represents two galvanometric scanning mirrors which work in synchronization to reflect the speckle images in a serpentine fashion over the entire CCD plane.

First, to better understand the four models, Figure 1 is included below as a diagram of the actual "box" which would be constructed. The sizes and distances in the diagram are not to scale.
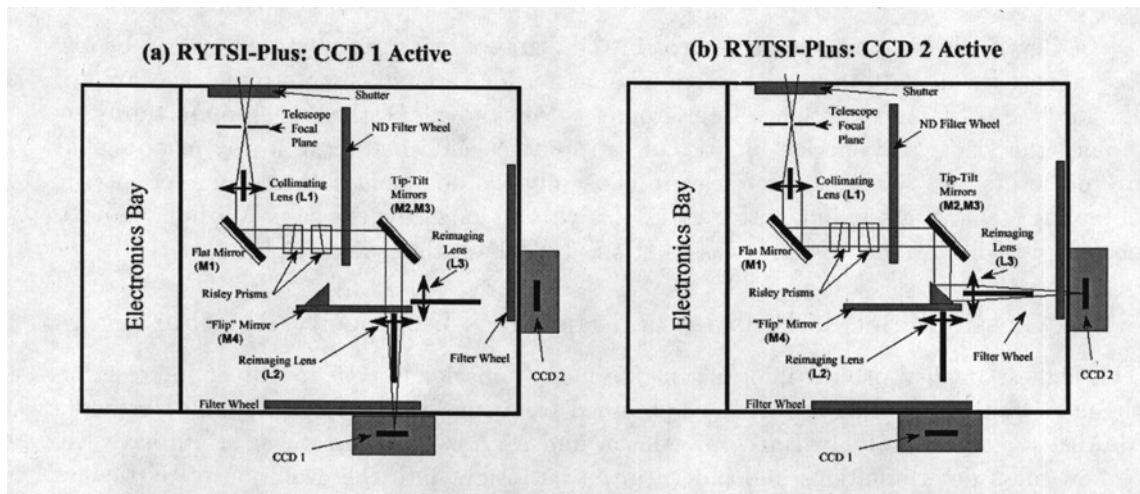
Figure 1: RYTSI-Plus Block Diagram (courtesy E. Horch)

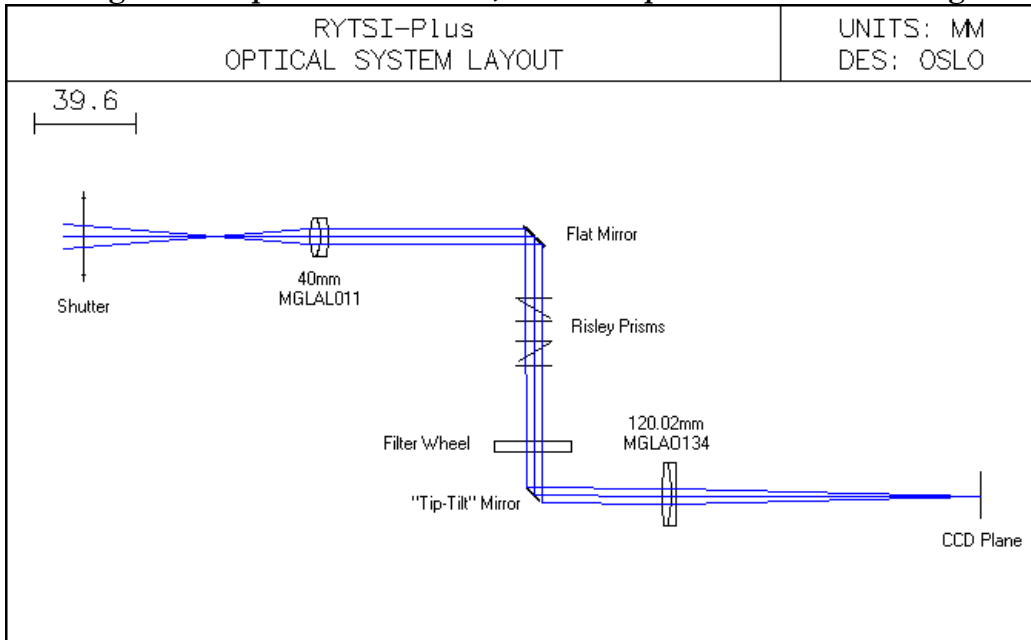**Figure 2: "flip" mirror <u>inactive</u>, and <u>no</u> "tip-tilt" raster mimicking**

RYTSI—Plus
OPTICAL SYSTEM LAYOUT

UNITS: MM
DES: OSLO

39.6

Shutter

40mm
MGLAL011

Flat Mirror

Risley Prisms

Filter Wheel

120.02mm
MGLA0134

"Tip-Tilt" Mirror

CCD Plane

Figure 3: "flip" mirror <u>inactive</u>, and "tip-tilt" raster mimicking (2.1° maximum raster angle)

RYTSI—Plus
OPTICAL SYSTEM LAYOUT

UNITS: MM
DES: OSLO

39.5
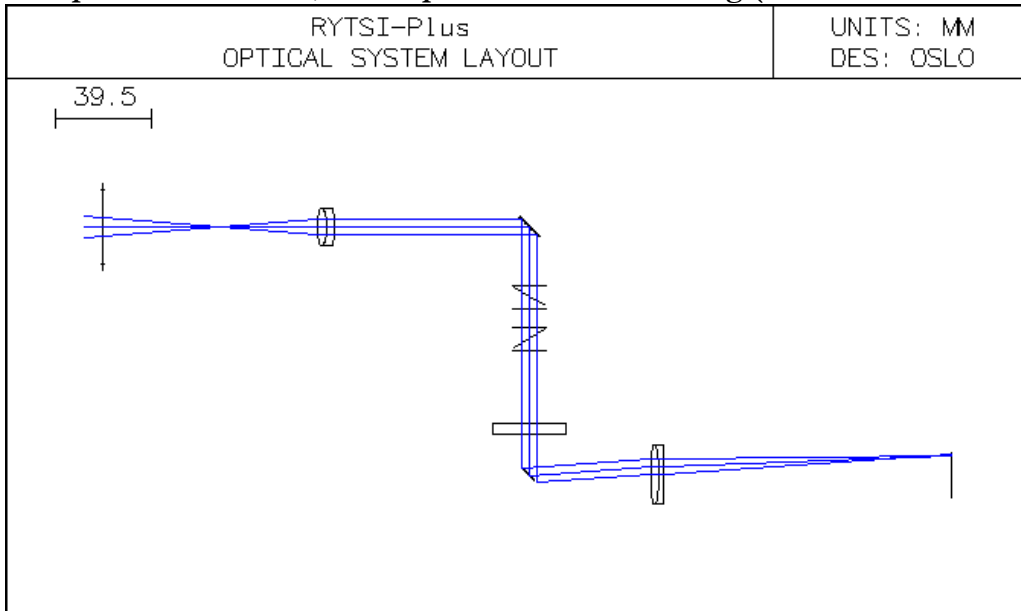
Figure 4: "flip" mirror <u>active,</u> and <u>no</u> "tip-tilt" raster mimicking

RYTSI—Plus
OPTICAL SYSTEM LAYOUT

UNITS: MM
DES: OSLO

58.4

40mm
MGLAL011

Risley Prisms

Filter Wheel

"Tip-Tilt" Mirror

"Flip" Mirror

120.02mm
MGLAO134

CCD Plane
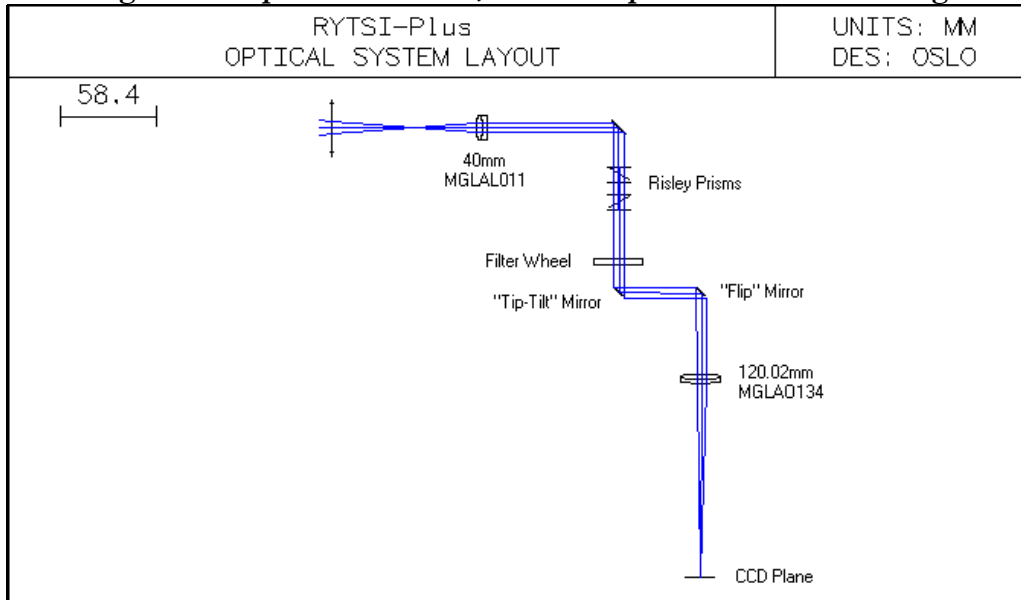
Figure 5: "flip" mirror <u>active,</u> and "tip-tilt" raster mimicking (1.4° maximum raster angle)

RYTSI—Plus
OPTICAL SYSTEM LAYOUT

UNITS: MM
DES: OSLO

58.2
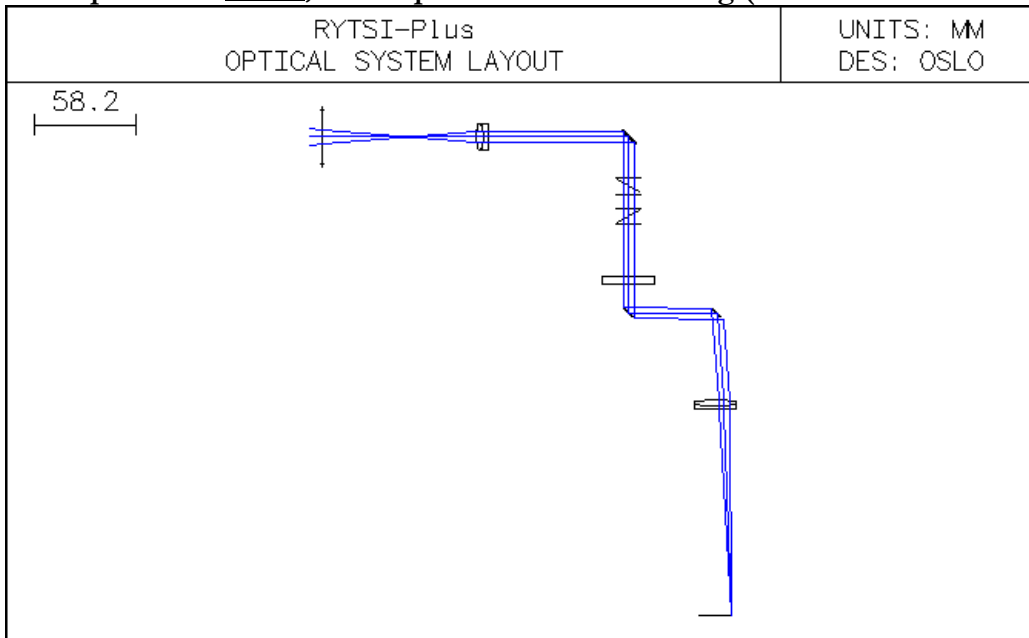
IMAGE PLANE ANALYSIS

POINT SPREAD FUNCTION COMPARISON

Figures 6a,b: "flip" mirror <u>inactive</u>, and <u>no</u> "tip-tilt" raster mimicking
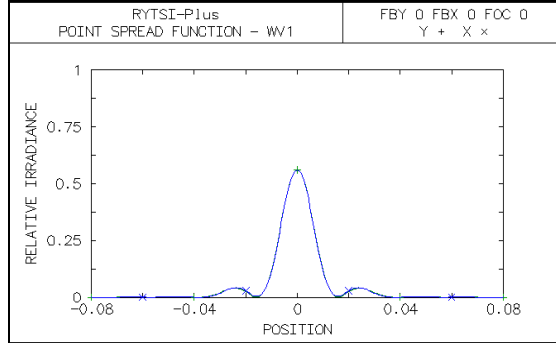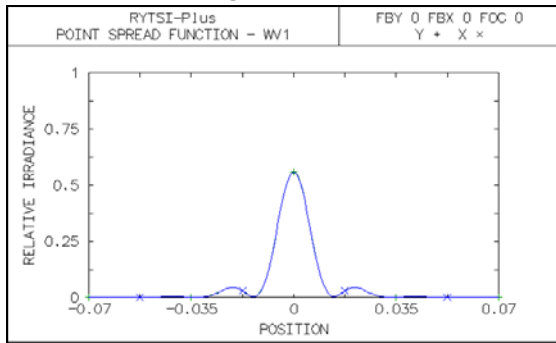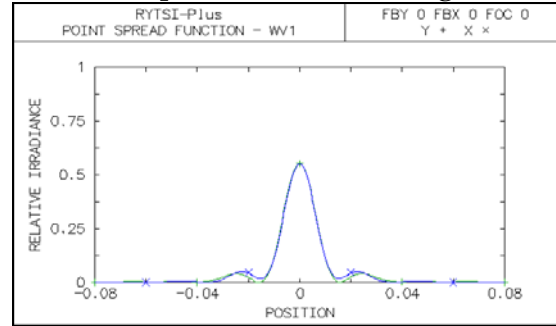

40mm / 120mm lens combination; maximum=0.5850   60mm / 180mm lens combination; maximum=0.5882

Figure 7a,b: "flip" mirror inactive, and "tip-tilt" raster mimicking

40mm / 120mm lens combination; maximum=0.4966   60mm / 180mm lens combination; maximum=0.5756

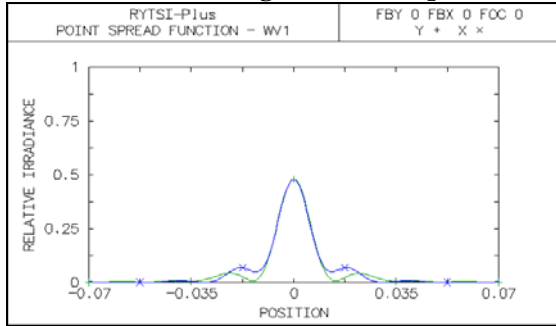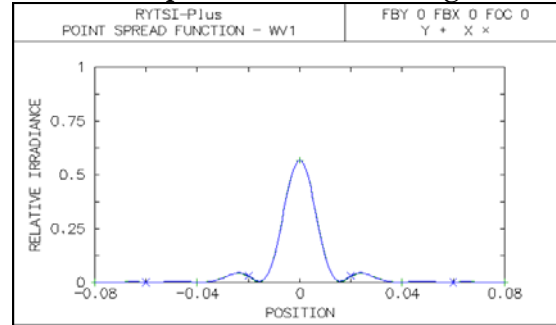**Figures 8a,b: "flip" mirror <u>active</u>, and <u>no</u> "tip-tilt" raster mimicking**

40mm / 120mm lens combination; maximum=0.5855   60mm / 180mm lens combination; maximum=0.5922
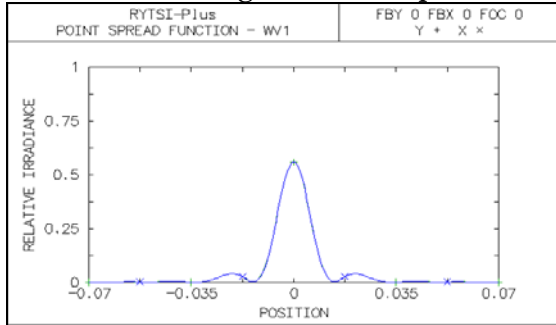
Figures 9a,b: "flip" mirror <u>active</u>, and "tip-tilt" raster mimicking

40mm / 120mm lens combination; maximum=0.4172   60mm / 180mm lens combination; maximum=0.5513
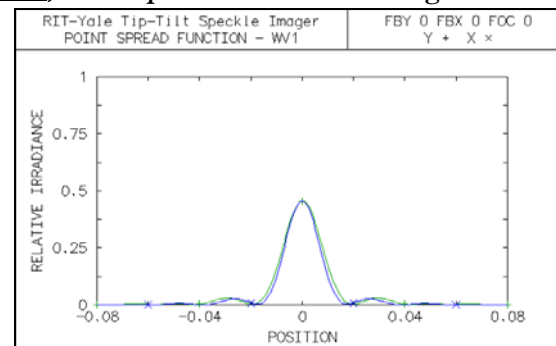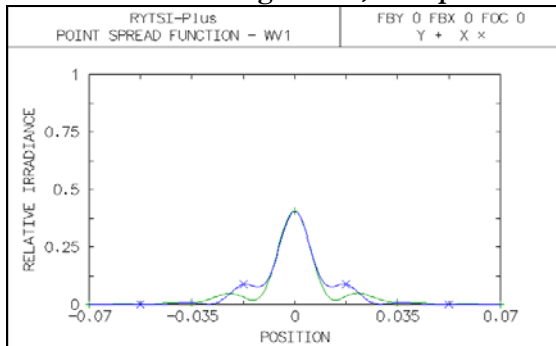
SPOT DIAGRAM COMPARISON

Figures 10a,b: "flip" mirror <u>inactive</u>, and <u>no</u> "tip-tilt" raster mimicking

RYTSI-Plus SPOT DIAGRAM	FBY 0 FBX 0 FOCUS 0	REFHT 0.6515 UNITS: mm

GEOMETRICAL SPOT SIZE 0.03142

GEOMETRICAL RMS Y SIZE 0.02223

DIFFRACTION LIMIT 0.01466

GEOMETRICAL RMS X SIZE 0.0222

RYTSI-Plus SPOT DIAGRAM	FBY 0 FBX 0 FOCUS 0	REFHT 0.9666 UNITS: mm

GEOMETRICAL SPOT SIZE 0.03612

GEOMETRICAL RMS Y SIZE 0.02578

DIFFRACTION LIMIT 0.0167

GEOMETRICAL RMS X SIZE 0.02529
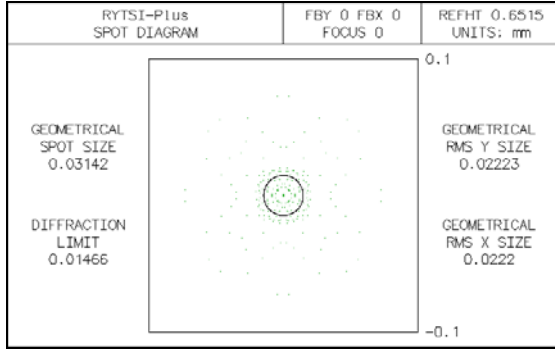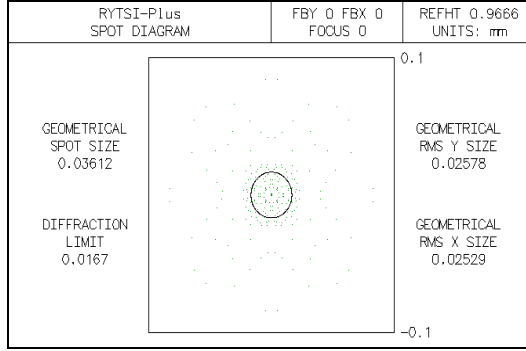
40mm / 120mm lens combination   60mm / 180mm lens combination

Figures 11a,b: "flip" mirror <u>inactive</u>, and "tip-tilt" raster mimicking

RYTSI-Plus SPOT DIAGRAM	FBY 0 FBX 0 FOCUS 0	REFHT 8.167 UNITS: mm

GEOMETRICAL SPOT SIZE 0.03166

GEOMETRICAL RMS Y SIZE 0.02438

DIFFRACTION LIMIT 0.0145

GEOMETRICAL RMS X SIZE 0.02019

RYTSI-Plus SPOT DIAGRAM	FBY 0 FBX 0 FOCUS 0	REFHT 7.55 UNITS: mm

GEOMETRICAL SPOT SIZE 0.03544

GEOMETRICAL RMS Y SIZE 0.02608

DIFFRACTION LIMIT 0.01667
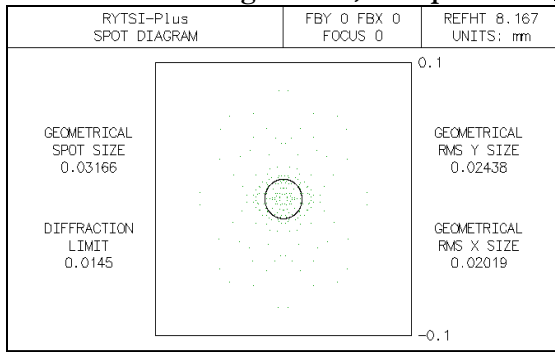
GEOMETRICAL RMS X SIZE 0.02399
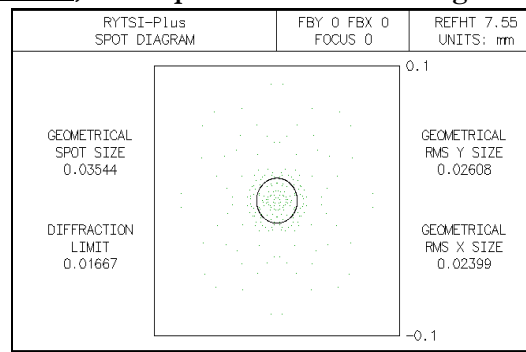
40mm / 120mm lens combination   60mm / 180mm lens combination

Figures 12a,b: "flip" mirror <u>active</u>, and <u>no</u> "tip-tilt" raster mimicking

RYTSI-Plus SPOT DIAGRAM	FBY 0 FBX 0 FOCUS 0	REFHT 0.648 UNITS: mm

GEOMETRICAL SPOT SIZE 0.03182

GEOMETRICAL RMS Y SIZE 0.02252

DIFFRACTION LIMIT 0.01457

GEOMETRICAL RMS X SIZE 0.02247

RYTSI-Plus SPOT DIAGRAM	FBY 0 FBX 0 FOCUS 0	REFHT 0.9803 UNITS: mm

GEOMETRICAL SPOT SIZE 0.03581

GEOMETRICAL RMS Y SIZE 0.02552

DIFFRACTION LIMIT 0.01688

GEOMETRICAL RMS X SIZE 0.02512
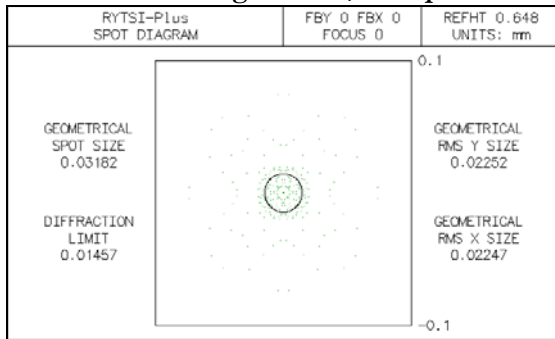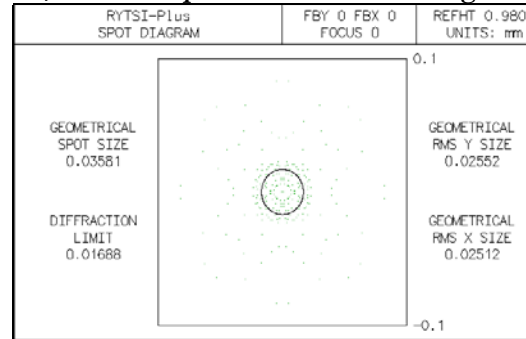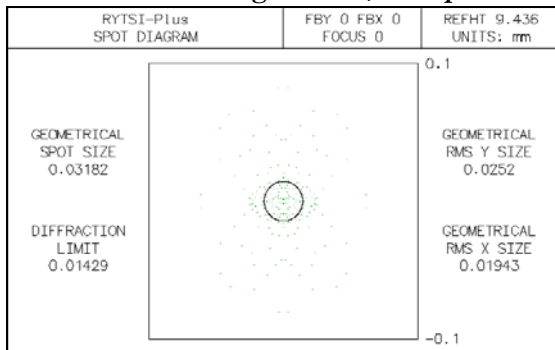
40mm / 120mm lens combination   60mm / 180mm lens combination

Figures 13a,b: "flip" mirror <u>active</u>, and "tip-tilt" raster mimicking

RYTSI-Plus SPOT DIAGRAM	FBY 0 FBX 0 FOCUS 0	REFHT 9.436 UNITS: mm

GEOMETRICAL SPOT SIZE 0.03182

GEOMETRICAL RMS Y SIZE 0.0252

DIFFRACTION LIMIT 0.01429

GEOMETRICAL RMS X SIZE 0.01943

RIT-Yale Tip-Tilt Speckle Imager SPOT DIAGRAM	FBY 0 FBX 0 FOCUS 0	REFHT 9.468 UNITS: mm

GEOMETRICAL SPOT SIZE 0.04296

GEOMETRICAL RMS Y SIZE 0.03219

DIFFRACTION LIMIT 0.01673

GEOMETRICAL RMS X SIZE 0.02844
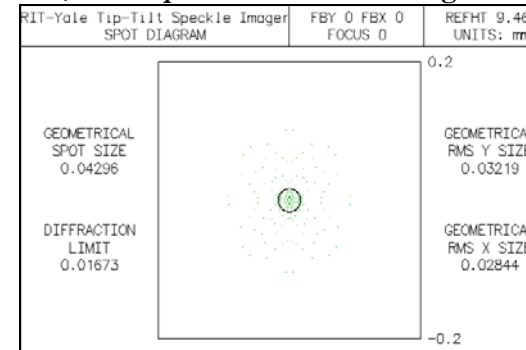
40mm / 120mm lens combination   60mm / 180mm lens combination

Discussion

Given the above data obtained from the OSLO® models, it has been determined that acceptable point spread functions and spot diagrams are obtained using the 40mm/120mm lens combination.

First, the term 'acceptable' must be defined. For non-raster mimicking cases, the maximum of the point spread functions must lie above 0.5 relative irradiance in order to be deemed 'acceptable.' For raster mimicking cases, the point spread function maximums must lie above 0.4 relative irradiance. Of course, the ideal point spread function would be a single spike at position=0 and corresponding to relative irradiance=1. However, in optical systems this is not possible, and given the expected performance of RYTSI-Plus, the above requirements for the acceptability of point spread functions have been defined. Second, by analyzing the spot diagrams, as stated earlier, the majority of the energy traveling through the equally spaced grid units on the entrance pupil, through the system and onto the CCD plane should lie within the diffraction limit (designated by the black circle in each plot). Sometimes, by analyzing the plot labels 'Geometric Spot Size' vesus 'Diffraction Limit,' the information does not describe the concentration of energy within the center diffraction-limited region. However, by comparing these two metrics, the differences between different models can be made, as well as the differences between each model and its respective 60mm/180mm comparison model.

Now that the definition of 'acceptable' point spread functions and spot diagrams has been defined, a comparison of image quality results can now be made between each individual final 40mm/120mm system models. Further, at the same time, it has been useful to study how image quality is affected by the choice of higher focal length lenses. Thus, a comparison can be made between results from the 40mm/120mm system and the respective results from the 60mm/180mm individual models. The maximum point spread function values, distinctly identified and labeled underneath the previous plots, prove that the distribution of energy is less blurred across the detector surface using the 60mm/180mm lens combination in RYTSI-Plus. In the "flip" mirror <u>inactive</u>, and <u>no</u> "tip-tilt" raster mimicking, Figures 6a,b, notice how the PSF reaches a maximum of 0.5850 in the 40mm/120mm model versus 0.5882 in the 60mm/180mm model. These results are well above the definition for acceptable. As the results also show, interestingly, that even higher PSF maximums were obtained from the "flip" mirror <u>active</u>, and <u>no</u> "tip-tilt" raster mimicking models, Figures 8a,b (0.5855 relative irradiance from the 40mm/120mm model versus 0.5922 relative irradiance from the 60mm/180mm model). The addition of the extra reflective surface, the "flip" mirror, should have yielded a lower PSF maximum. Both PSF maximums are nearly equal and lie well above the required acceptability level. Notice in both raster-mimicking models, Figures 7a,b and Figures 9a,b, the PSF maximums are much lower than results from their respective on-axis models. This shows that, as the "tip-tilt" mirror move the image in a serpentine fashion across the image plane, the image quality will be best at the center and degrade significantly as the angle of the "tip-tilt" mirror is increased towards the corners of the CCD.

The results from the spot diagram analysis becomes less clear as we compare the 40mm/120mm models versus the 60mm/180mm models. Indeed, in all cases, as shown by Figures 10 through 13, the majority of the distribution of energy lies within the diffraction limit. Analyzing the spot diagrams at an enlarged scale closely, one can tell that indeed more energy lies within the diffraction limit in the 60mm/180mm models versus the respective 40mm/120mm models.

Conclusions

As a result of this project, it has been determined that **acceptable** point spread functions and spot diagrams result from the use of a 40mm collimating lens and a 120mm reimaging lens for the on-axis, "flip" mirror active, and raster-mimicking models. As expected, <u>better</u> point spread functions and spot diagrams resulted when modeling the system with a 60mm collimating lens and a 180mm reimaging lens; however, since strict spatial constraints have been placed on the size of RYTSI-Plus and the housing must be kept to a limited size, a 40mm collimating lens and 120mm reimaging lens will be employed in the future construction process.

References

E. Horch, "Proposal to the NSF for RYTSI-Plus Funding," pp. 1-15.

E. P. Horch, Z. Ninkov, R. D. Meyer and W. F. van Altena [2001], "RYTSI: A New Way to Do Speckle Imaging," *Bulletin of the American Astronomical Society*, **33**, pp. 790-791.

E. Horch, Z. Ninkov and W. F. van Altena [1998], "A New Low-Noise High- Quantum-Efficiency Speckle Imaging System," *Proc. SPIE*, **3355**, pp. 777-785.